Microbiological-enhanced mixing across scales during *in-situ* bioreduction of metals and radionuclides at Department of Energy Sites

A. J. Valocchi (PI), C.J. Werth, W-T. Liu, R. Sanford, *U.of Illinois Urbana-Champaign*, K. Nakshatrala, *U. of Houston*,

Final Project Report

Executive Summary

Bioreduction is being actively investigated as an effective strategy for subsurface remediation and long-term management of DOE sites contaminated by metals and radionuclides (i.e. U(VI)). These strategies require manipulation of the subsurface, usually through injection of chemicals (e.g., electron donor) which mix at varying scales with the contaminant to stimulate metal reducing bacteria. There is evidence from DOE field experiments suggesting that mixing limitations of substrates at all scales may affect biological growth and activity for U(VI) reduction.

Although current conceptual models hold that biomass growth and reduction activity is limited by physical mixing processes, a growing body of literature suggests that reaction could be enhanced by cell-to-cell interaction occurring over length scales extending tens to thousands of microns. Our project investigated two potential mechanisms of enhanced electron transfer. The first is the formation of single- or multiple-species biofilms that transport electrons via direct electrical connection such as conductive pili (i.e. 'nanowires') through biofilms to where the electron acceptor is available. The second is through diffusion of electron carriers from syntrophic bacteria to dissimilatory metal reducing bacteria (DMRB). The specific objectives of this work are i) to quantify the extent and rate that electrons are transported between microorganisms in physical mixing zones between an electron donor and electron acceptor (e.g. U(IV)), ii) to quantify the extent that biomass growth and reaction are enhanced by interspecies electron transport, and iii) to integrate mixing across scales (e.g., microscopic scale of electron transfer and macroscopic scale of diffusion) in an integrated numerical model to quantify these mechanisms on overall U(VI) reduction rates.

We tested these hypotheses with five tasks that integrate microbiological experiments, unique microfluidics experiments, flow cell experiments, and multi-scale numerical models. Continuous fed-batch reactors were used to derive kinetic parameters for DMRB, and to develop an enrichment culture for elucidation of syntrophic relationships in a complex microbial community. Pore and continuum scale experiments using microfluidic and bench top flow cells were used to evaluate the impact of cell-to-cell and microbial interactions on reaction enhancement in mixing-limited bioactive zones, and the mechanisms of this interaction. Some of the microfluidic experiments were used to develop and test models that considers direct cell-to-cell interactions during metal reduction. Pore scale models were incorporated into a multi-scale hybrid modeling framework that combines pore scale modeling at the reaction interface with continuum scale modeling. New computational frameworks for combining continuum and pore-scale models were also developed

Experimental Microbiology: Developing a system of syntrophs and metal reducers

When introduced to groundwater, heavy metals can persist through sorption to mineral surfaces and biofilms. Indigenous metal-reducing microorganisms (MRB) are thought to accomplish natural attenuation of groundwater heavy metal pollution, by degrading dissolved organic compounds and respiring the heavy metals (e.g., selenium and uranium), whereby converting the heavy metals to a very poorly soluble state. However, for metals adsorbed to surfaces in mixing-limited pores, MRB may have limited access to energy sources dissolved in the bulk groundwater flow. As a novel remediation strategy, we are investigating microorganisms that may degrade energy sources available in the bulk groundwater flow and transfer metabolic byproducts to MRB in mixing-limited pores for downstream attenuation of mobile heavy metal species. Two possible modes of delivery are (a) electron-carrying metabolite transfer through diffusion and (b) direct electron transfer through microbial nanowires (Fig. 1B). "Syntrophs" are particularly attractive for this remediation strategy as they are adapted to degrading low-energy compounds and symbiotically providing metabolic byproducts to partner organisms under anaerobic conditions.

Although syntrophs are ideal for this remediation strategy, the mechanism for metabolite transfer to the partner organism (MRB in this case) is still unclear. Cultivation experiments on *Syntrophobacter wolinii* strain DB, a representative syntroph, with *Geobacter sulfurreducens* strain PCA, a representative MRB, suggested that syntrophs may transfer H_2 to MRB for metal reduction. Additional experiments with mutant *G. sulfurreducens* strain PCA lacking H_2 metabolism (specifically the hyb) and microscopy further supported the possibility that H_2 may be the key mechanism for energy transfer between syntrophs and MRB. To complement these cultivation-based studies in elucidating the metabolic and symbiotic capacity of syntrophs, we are currently sequencing the genomes of ten syntrophs strongly associated with anaerobic environments.

Analysis of the genome of *Syntrophorhabdus aromaticivorans* strain UI, a syntroph often found in polluted groundwater, (recently published: Nobu et al., 2014, *Environmental Microbiology*) and all other previously published syntroph genomes revealed novel genes that may contribute to a unique mechanism for H_2 production and transfer to symbiotic partners. Further, based on careful genomic analysis, we also identified that syntrophs most likely employ an unknown electron carrier to facilitate their symbiotic lifestyle. This clearly demonstrated that genomics is an effective and complementary approach to cultivation-based experiments in investigating potential interaction between syntrophs and MRB. Thus, we believe that further investigation of the newly sequenced syntroph genomes will provide essential insight into their behavior.
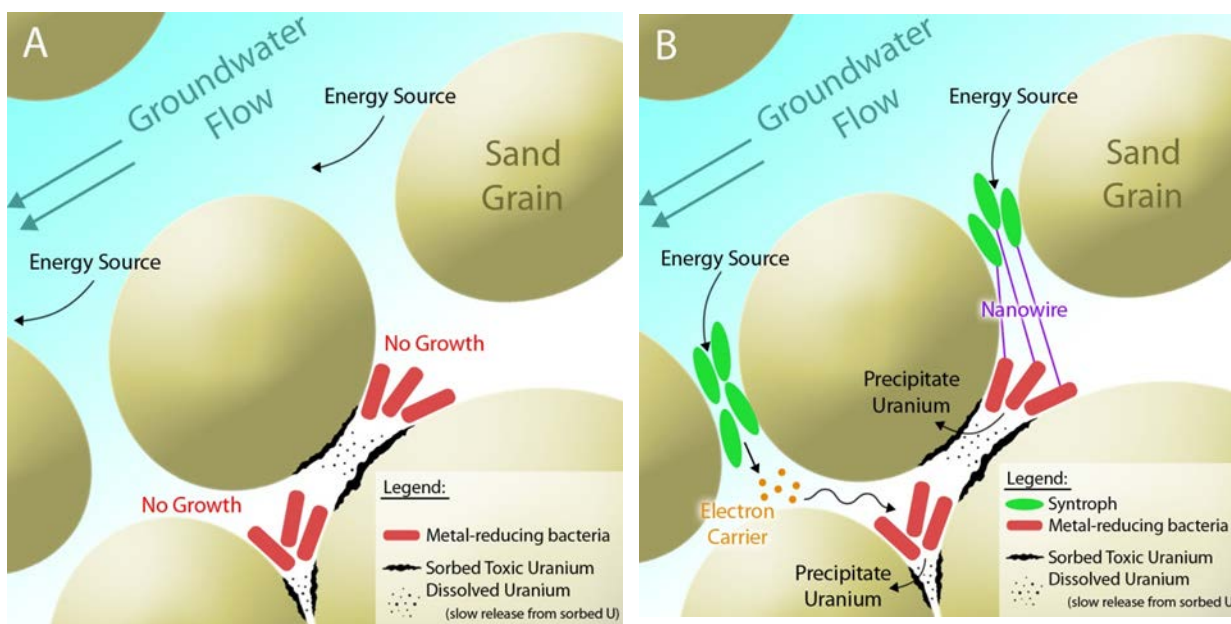
Figure 1. Communication between bulk groundwater flow and isolated pore space mediated by syntroph-MRB interactions. When groundwater is amended with chemical energy sources to stimulate groundwater uranium bioremediation, the energy source cannot be delivered to mixing-limited pores. (a) When only MRB is present/stimulated, the energy source flowing in the bulk groundwater flow does not reach MRB associated with uranium adsorbed in mixing-limited pore space. (b) When syntrophs and MRB are interacting, the syntroph can interact with the bulk groundwater flow, assimilate the energy source, and pass energy to the MRB in the mixing-limited pores. The two major theoretical mechanisms for this energy transfer are electron carriers and nanowires. Syntrophs may (i) secrete chemical or protein electron carriers to pass energy to MRB through diffusion or (ii) directly connect to MRB and shuttle electrons to MRB.

In investigating potential energy transfer between syntrophs and MRB, it is also necessary to understand how syntrophs convert environmentally available organic compounds to transferrable energy. Analysis of the *S. aromaticivorans* strain UI genome revealed novel mechanisms for conversion of aromatic compounds to H_2. To complement this study, we will also investigate syntrophic degradation of propionate (*Syntrophobacter wolinii*), butyrate (*Syntrophomonas palmitatica* and *S. bryantii*), alcohols (*Tepidanaerobacter syntrophicus*), aromatic compounds (*Sporotomaculum syntrophicus*), and amino acids (*Eubacterium acidaminiophilum*, *Caloramator proteoclasticus*, and *Acidaminobacter hydrogenoformans*). Exploration of these syntroph genomes will provide essential insight into how syntrophs may produce H_2 from various organic compounds to symbiotically interact with MRB in subsurface heavy metal remediation sites. In order to ensure generation of complete and high quality genomes for comprehensive analysis, we employ cutting-edge MiSeqv3 Illumina technology and bioinformatics software (e.g., SPAdes and Trimmomatic) for corresponding genome sequencing and assembly.

Experimental Microbiology: Evaluating the rate of solid phase metal reduction by dissimilatory metal reducing bacteria

Experiments were conducted to characterize the kinetics of a common MRB for solid phase metal reduction under different environmental conditions. *Geobacter sulfurreducens* strain PCA was used as a model MRB in kinetic experiments conducted in a flow-through reactor, with solid manganese dioxide (MnO_2) as the electron acceptor and acetate as the electron donor. A flow-through system was chosen for the experiments to allow for the evaluation of transport mechanisms that are not present in batch reactors. The MnO_2 was coated on glass substrates in the reactor, and the rate of reduction was evaluated by measuring Mn^{2+} in the effluent solution.

The first condition evaluated experimentally was the impact of different flow rates on the reduction kinetics of MnO_2 by G. *Sulfurreducens*. High flow conditions showed a steeper slope for the cumulative mass of manganese (Mn^{2+}) in the effluent per time (Figure 2), which suggests a faster reduction rate under high flow conditions. A simple numerical model based on a single Monod reaction term was created and used to fit the half saturation constant in the Monod equation. Assuming the same initial biomass, yield, and maximum specific growth rate for each experiment, the half saturation constant was determined to be 0.05 mmol under low flow (5 mL/hr) conditions and 0.01 mmol under high flow (50 mL/hr) conditions.
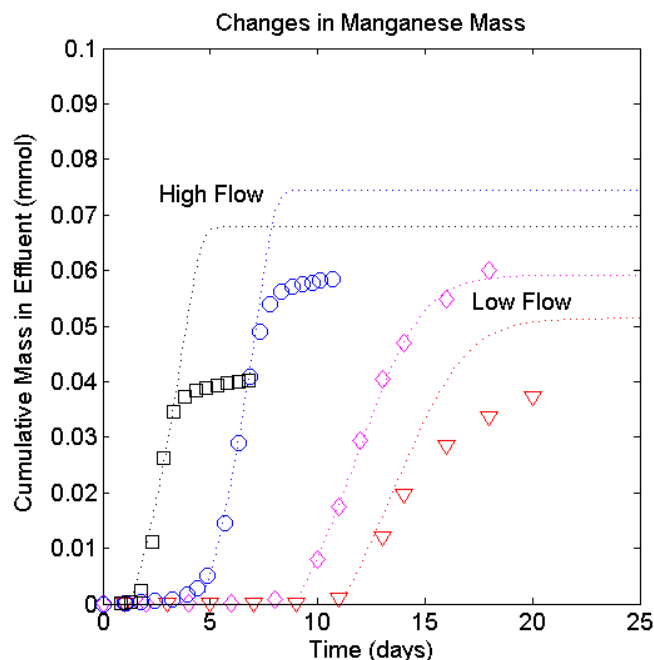
It is possible that the mass in the effluent is impacted by the diffusion of acetate to the surface of the MnO_2. Under high flow conditions, the boundary layer will be smaller, possibly allowing faster mass transfer, and an apparent faster reduction rate. A model that incorporates diffusion is necessary to evaluate this.

Ongoing MRB reduction kinetics experiments involve evaluating the impact of electron shuttles on the rate of MnO_2 reduction, and altering the experimental method to obtain a more complete mass balance. After characterizing the reduction kinetics of MRB, a combined system can be better evaluated.

Figure 2. Results from flow through experimental reactor for reduction of solid phase MnO_2 by G. *Sulfurreducens*.

Micro-fluidics Experimental Work: Understanding electron transfer in flowing systems

The main objective of the microfluidics experiments is to elucidate the role of extracellular electron transfer (EET) via microbial nanowires and electron shuttling in uranium reduction by dissimilatory metal-reducing bacteria. Experimental parameters such as pH and groundwater velocity reflect actual measurements taken at major sites of contamination including the Rifle and Oak Ridge Integrated Field Sites. Results are intended to provide clear, quantitative data at a mechanistic level that may be used to design of cost-effective bioremediation strategies exploiting the natural ability of certain species of bacteria to reduce metals. The following hypotheses are related to the microfluidics experiments:

1. Dissimilatory metal-reducing bacteria can directly reduce metals at micrometer scales across a nanoporous physical barrier that allows the passage of nanowires but not whole cells.

2. Concentration thresholds for the production of nanowires and electron shuttles can be determined by exposing cells to concentration gradients of electron donor and acceptor.

3. The high energetic cost of producing electron shuttles will limit their synthesis under higher flow rates, leading to increased reliance on nanowires to reduce metals when not in direct contact with the cell.

Experiments were conducted using synthetic birnessite, a poorly crystalline form of manganese dioxide (MnO_2) found in nature existing in the Mn(IV) oxidation state. Its rapid reduction from Mn(IV) to Mn(II) by bacteria make it a convenient surrogate for more environmentally relevant contaminants such as U(VI) or Cr(VI) that are reduced at much slower rates due to their toxicity. This has allowed for the modification of experimental procedures and the development of new protocols in a reasonable time frame. Mn(IV) is reduced by the same pathway as uranium making it a true surrogate. Furthermore, its insoluble nature can be exploited to accurately test the rate and scale of nanowire reduction independent of diffusion by constructing a physical barrier to insoluble material. This barrier is designed to allow passage of bacterial nanowires while preventing passage of Mn(IV) particles and bacteria. *Geobacter sulfurreducens* and *Shewanella oneidensis* MR-1, two species of dissimilatory metal-reducing bacteria, were selected because of their proven ability to reduce metals by EET, ubiquitous presence at contaminated sites, and metabolic diversity that includes the use of both U(VI) and MnO_2 as terminal electron acceptors.

We designed and fabricated silicon-based microfluidic reactors to investigate long-range EET under conditions that simulate a groundwater environment. The versatility of these reactors has allowed us to determine whether nanowires are required by *Geobacter sulfurreducens* for long-range EET, how deeply their nanowires may penetrate nanopores, and what role redox cofactors like riboflavin have in transferring electrons to solid electron acceptors. A picture of one of these reactors is shown below in Figure 3a, accompanied by an SEM image of the nanoporous wall in Figure 3b that is comprised of a series of pillars. The spacing between pillars is < 200 nm, small enough to prevent bacteria from penetrating the wall yet large enough to allow passage of nanowires and electron shuttles.

Figure 3: A picture of the microfluidic reactor (left) showing experimental conditions, and an SEM image of the physical barrier (right) that separates the center region where the two channels meet.

Experiments to date indicate that metal reduction only occurred under reduced conditions, even if bacteria were put into direct contact with the metal. Chemical reductants like sulfide or cysteine are commonly used in batch experiments to lower the redox potential of the medium, but abiotic reduction of MnO_2 was observed when they were continuously infused. Our solution was to infuse a secondary bacteria that lowers the redox potential by selectively reducing oxygen. We chose *E. coli* K-12 based on its demonstrated ability to grow in co-culture with *G. sulfurreducens*, rapidly lower the redox potential, and excrete metabolites that act as redox buffers against oxygen intrusion. By providing *E. coli* with glucose, we avoided metabolic overlap and therefore competition with *G. sulfurreducens*. Controls indicated that *E. coli* did not oxidize acetate, reduce MnO_2, or inhibit the metabolic activity of G. *sulfurreducens*.

Despite anaerobic conditions, favorable redox potential, and no mass transfer limitations in relation to electron donor, *G. sulfurreducens* was unable to reduce MnO_2 across the nanoporous wall even after 2 months of continuous operation. However, MnO_2 was completely reduced in the reactor when cells were infused on the same side as MnO_2, putting them into direct contact with the metal. This indicated that conditions inside the reactor were favorable for metal reduction, but not for long-range EET. We decided to add 100 nM riboflavin based on recent evidence that flavins are required for terminal elec-

tron transfer from the cytochromes to the solid metal surface. In the case of *G. sulfurreducens*, these flavins are strongly adsorbed to the cytochromes present on the outer membrane and nanowire surface. Upon addition of riboflavin, MnO_2 was reduced across the nanoporous wall within 5 days to $MnCO_3$ as shown in Figure 4. Reduction appeared to stop 10-15 microns beyond the nanoporous wall, consistent with AFM and TEM measurements that show nanowires extending up to 20 microns in length. While the presence of riboflavin was essential for long-range EET, addition of riboflavin in serum bottles resulted only in modest improvement of reduction rates.
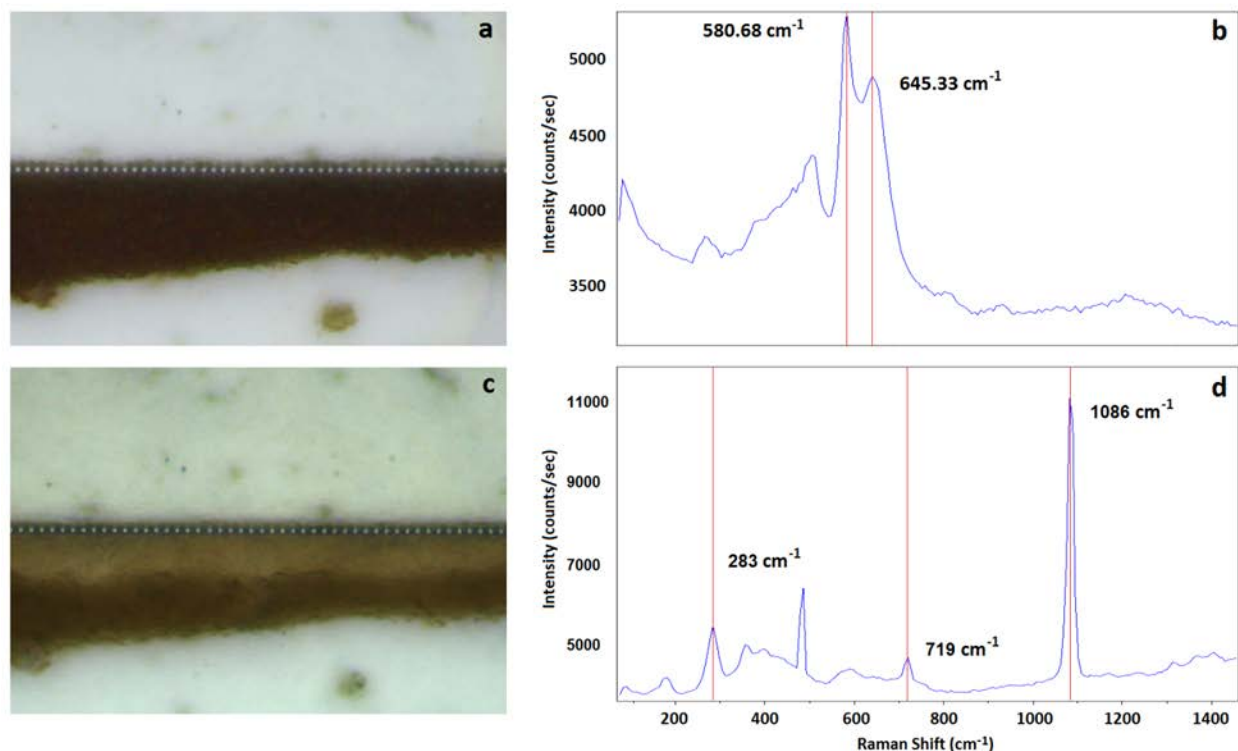

Figure 4: MnO_2 (a) and its characteristic Raman shift (b) measured inside the reactor. After 5 days, MnO_2 was biologically reduced to $MnCO_3$ (c, lighter color), which was confirmed by Raman spectroscopy (d).

Fluorescence microscopy was used to look for accidental cell passage across the nanoporous wall. The c-type cytochromes involved in EET naturally fluoresce with a DAPI filter under reduced conditions (Figure 5a), allowing us to map the location of cells during an experiment and also determine the onset of reduced conditions. Upon completion of the experiment, dilute acid is infused to dissolve reduced products and kill cells. The reactor is incubated with propidium iodide to stain dead bacteria, providing us with an additional method to check for accidental passage across the wall. As shown in Figure 5b, all cells remained on one side of the reactor.
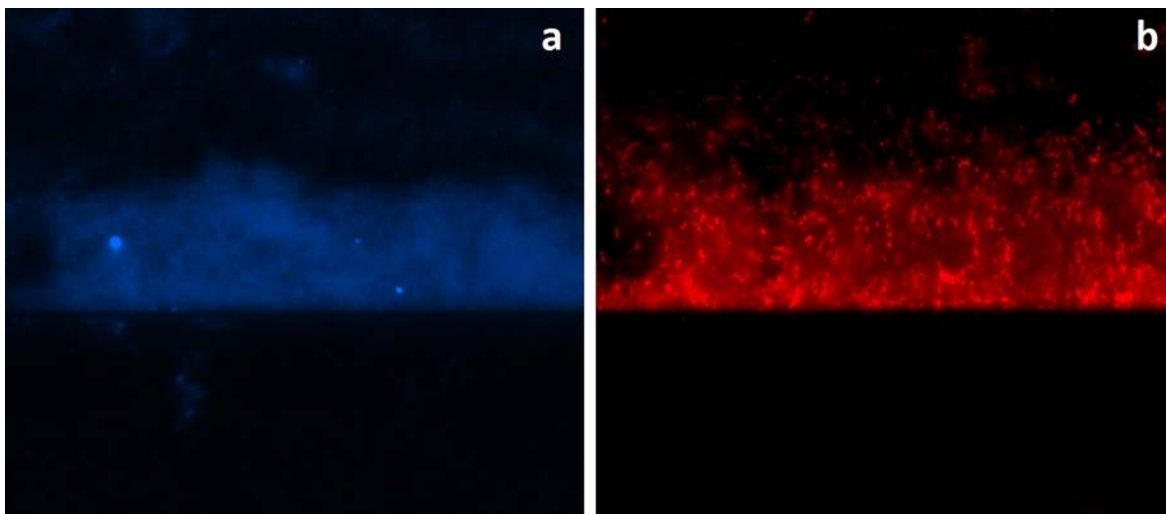
Figure 5: Autofluorescence of c-type cytochromes on *G. sulfurreducens* KN400 under DAPI at the onset of reduced conditions (a), and dead cell staining with propidium iodide after acid infusion (b). Note the absence of cells across the centerline, indicating no bacterial passage across the nanoporous wall.

The requirement of nanowires for long-range EET was tested using *G. sulfurreducens* KN400 grown at 31°C ± 1°C. Pili assembly is prevented at temperatures exceeding 30°C, resulting in a nanowire-deficient wild-type strain. Growth on MnO_2 in serum bottles showed no inhibition of metal reduction by growth at higher temperature; in fact, reduction occurred 20 percent faster. Reduction was also observed in the microfluidic reactors when cells were in direct contact with the MnO_2. However, long-range EET across the wall was completely inhibited, even after 9 days of operation as shown in Figure 6. This result indicates that nanowires may not be necessary for reduction of insoluble electron acceptors when in direct contact, but are required for EET.
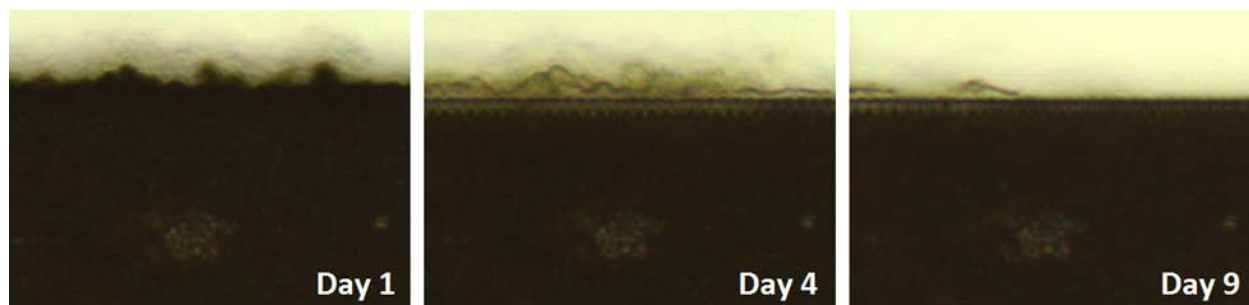

Figure 6: Progression of MnO_2 reduction by *G. sulfurreducens* KN400 grown at 31°C ± 1°C. MnO_2 that had bypassed the wall was reduced, but long-range EET was not observed even after 9 days.

We are currently investigating the requirement of nanowire conductivity in long-range EET using *G. sulfurreducens* Aro5, a mutant strain expressing nanowires with proper decoration of cytochromes, but significantly diminished conductivity. We are also in the preliminary stages of experiments designed to investigate the effect of flow rate on EET mechanism using *S. oneidensis* MR-1, and the concentration threshold for nanowire and electron shuttle expression using selenite as a surrogate for soluble U(VI).

Micro-fluidics Experimental Work: Contaminant fate in the mixing zone

Uranium can be immobilized through two pathways. First, U(VI) can be biologically reduced to uraninite (UO_2), a precipitate. Second, the product of biological sulfate reduction, sulfide, can abiotically reduce U(VI) to UO_2. To understand how the two pathways contribute to uranium immobilization in the mixing zone, we conducted an experiment and used selenium as a surrogate for uranium because the immobilization of selenium follows the two similar pathways, but selenium is much easy to work with in the lab. In the first pathway, selenite is biologically reduced to elemental selenium (Se^0). In the second pathway, sulfide abiotically precipitates with selenite to form selenium sulfides (Se_nS_{8-n}). Using selenium instead of uranium has another advantage since the end selenium products of two pathways are different, which makes it possible to distinguish the two pathways.

As shown in Figure 7 below, a microfluidic flow cell experiment was conducted to mimic the mixing zone in a site contaminated by selenite. The dimensions of the flow cell were 2 cm (length) × 1 cm (width) × 20 µm (height). The flow cell contained a homogeneous pore network that consisted of a uniform distribution of 300-µm-diameter cylindrical posts. Mineral salts solution containing selenite and sulfate was supplied at the top inlet, and mineral salts solution containing propionate and sulfate was supplied at the bottom inlet. The experiment showed that red particles of amorphous elemental selenium precipitate on the selenite-rich side of the mixing zone, while long crystals of selenium sulfides precipitate on the propionate-rich side of the mixing zone. We developed a continuum-scale reactive transport model that considers both pathways and inter-species electron transport. Acetate is the main electron carrier that transports electrons from propionate to selenite-reducing bacteria. The simulated results are consistent with the experimental results, and indicate that spatial segregation of the two selenium precipitates is due to the segregation of the more thermodynamic favorable selenite reduction and the less thermodynamically favorable sulfate reduction. The results also demonstrate that both pathways significantly contribute to selenite immobilization. If parameters for biotic and abiotic uranium reduction is available in the future, the same model can be used to quantify the contribution of the two pathways. This work was reported in Tang et al. (2015b)
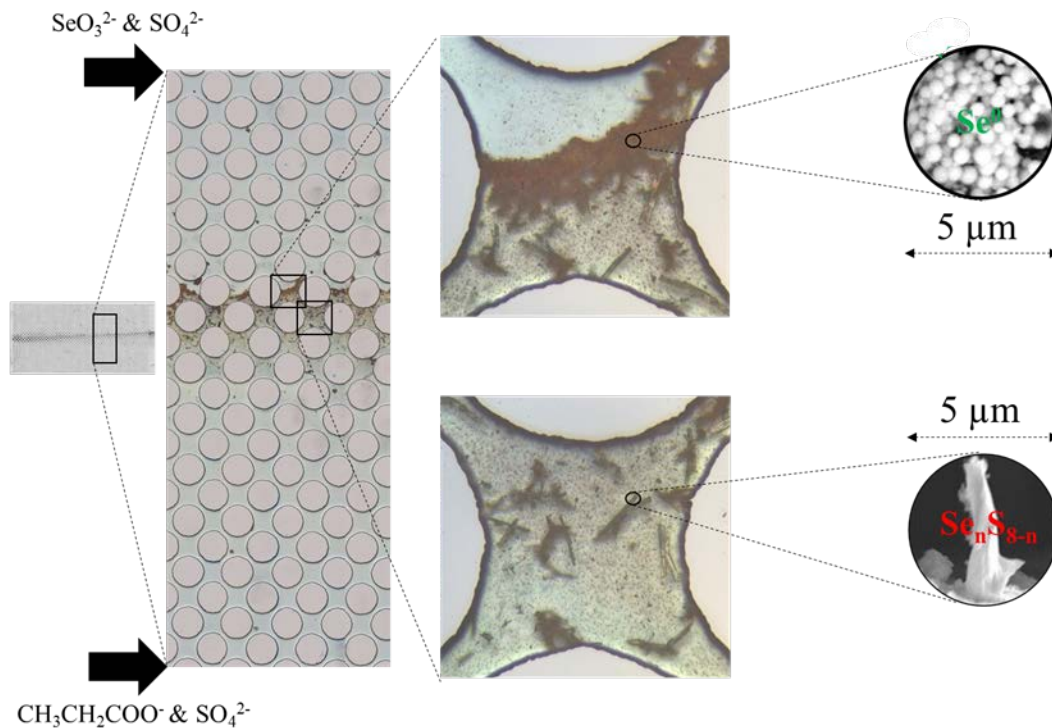

Figure 7. Segregation of the elemental selenium (Se^0) and selenium sulfides (Se_nS_{8-n}) in the mixing

Modeling Work: Multi-species biofilm dynamics and metal reduction and feedback with flow

The overall objective of the modeling work is to develop a pore-scale model that considers direct cell-to-cell interactions during U(VI) reduction and then incorporate the pore-scale model into a multi-scale hybrid model that combines pore scale modeling at the reaction interface with continuum scale modeling. We take the following five tasks to achieve this overall objective:

1) Improving a pore-scale, single-species biofilm model that we previously developed.
2) Improving a cellular automaton method to model multispecies biofilm.
3) Using the improved pore-scale biofilm from step 1 and the improved multispecies biofilm modeling method from step 2 to develop a pore-scale model that considers direct cell-to-cell interactions during U(VI) reduction; this model considers inter-species electron transfer.
4) Incorporating direct electron transfer (i.e., through nanowires) into the multispecies biofilm model.
5) Developing a multi-scale hybrid model that combines the pore-scale modeling in step 4 with continuum scale modeling.

We have completed tasks 1-3 and published the work in two journal papers (Tang and Valocchi, 2013; Tang et al., 2013). Also, we have completed part of tasks 4 and 5. Below we briefly summarize the work in each task.

1) We developed a pore-scale biofilm model that solves the flow field using the lattice Boltzmann method, the concentration field of chemical species using the finite difference method, and biofilm development using the cellular automaton method. We adapt the model from a previous work and expand it by implementing biofilm shrinkage in the cellular automaton method. The new pore-scale biofilm model is then evaluated against a previously published pore-scale biofilm experiment, in which two micro-fluidic flow cells, one with a homogeneous pore network and the other with an aggregate pore network, were tested for aerobic degradation of a herbicide. The simulated biofilm distribution and morphology, biomass accumulation, and contaminant removal are consistent with the experimental data. Biofilm detachment in this model occurs when the local shear stress is above a critical value; this critical shear stress is the only adjustable parameter in the model. We use the critical value from our previously published modeling study and find it works well in this case with different pore networks and microbial species. We also use the model to show that the interaction between flow and biofilm growth is important to predict contaminant removal. The computational time of the new model is reduced 90% compared to our prior work due to implementation of biofilm shrinkage in the cellular automaton method. To the best of our knowledge, this is the first time that biofilm shrinkage has been incorporated into a pore-scale model for simulation of pollutant biodegradation in porous media. This is reported in Tang et al. (2013).

2) We proposed an improved cellular automaton method to simulate multispecies biofilm. Biomass-spreading rules used in previous cellular automaton methods to simulate multispecies biofilm introduced extensive mixing between different biomass species or resulted in spatially discontinuous biomass concentration; this caused results based on the cellular automaton methods to deviate from experimental results and those from the more computationally intensive continuous method. To overcome the problems, we propose new biomass-spreading rules in this work: Excess biomass spreads by pushing a line of grid cells that are on the shortest path from the source grid cell to the destination grid cell, and the fractions of different biomass species in the grid cells on the path change due to the spreading. To evaluate the new rules, three two-dimensional simulation examples are used to compare the biomass distribution computed using the continuous method and three cellular automaton methods, one based on the new rules and the other two based on rules presented in two previous studies in the literature. The relationship between the biomass species is syntrophic in one example and competitive in the other two examples. Simulation results generated using the cellular automaton

method based on the new rules agree much better with the continuous method than do results using the other two cellular automaton methods. The new biomass-spreading rules are no more complex to implement than the existing rules. This is reported in Tang and Valocchi (2013).

3) We developed a pore-scale model that considers direct cell-to-cell interactions during U(VI) reduction. The model framework was adapted from the pore-scale, single-species biofilm model in task 1, but we extended it to a multi-species model using the improved cellular automaton method in task 2. This model has three biomass species (syntrophs, dissimilatory metal reducing bacteria (DMRB), and inert biomass) and four chemical species (propionate, acetate, hydrogen, and U(VI)). Syntrophs oxidize propionate to acetate and hydrogen, which are used as electron donors by DMRB to reduce U(VI) to U(IV). Figure 8 shows the simulated data in a micro-fluidic flow cell on the 100th day. DMRB mainly grow along the centerline of the flow cell, where U(IV) mixes with H_2 and acetate. Syntrophs mainly grow at the lower inlet and the along the centerline, where the concentration of propionate is high, but the concentrations of H_2 and acetate are low.

(a) Flow cell

(b) Flow + biomass (mol $C_5H_7O_2N/m^3$)

(c) Biomass distribution
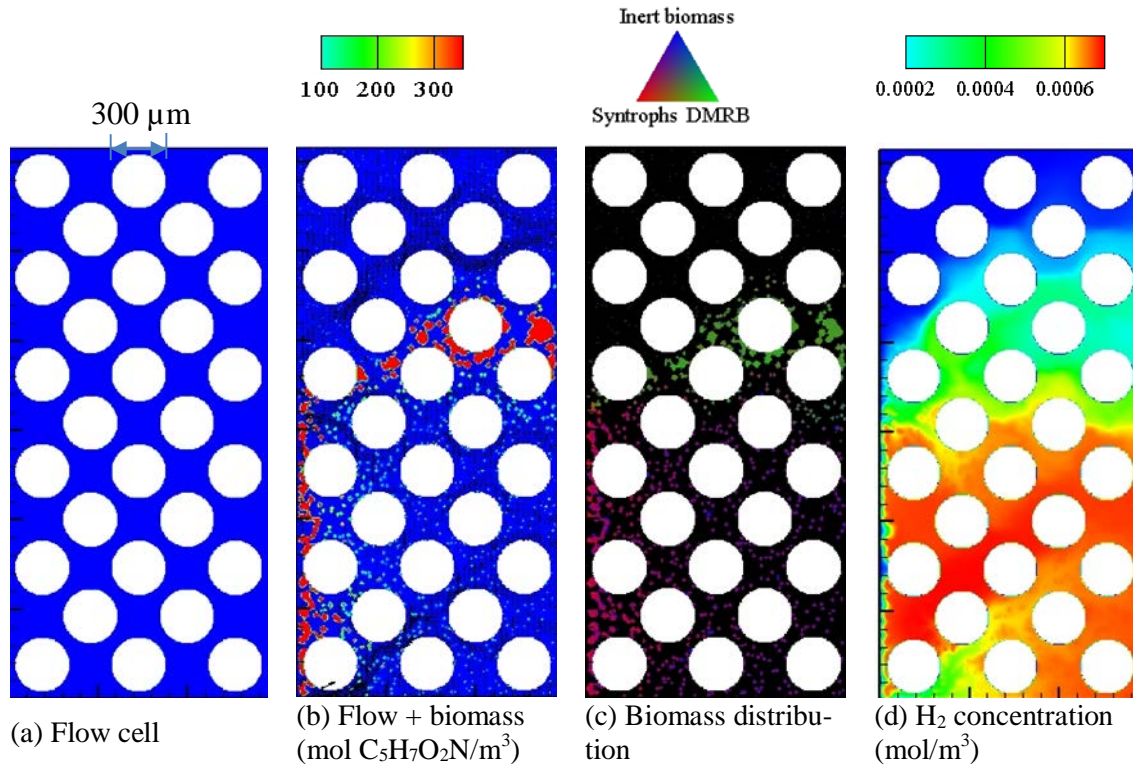
(d) H_2 concentration (mol/m^3)

Figure 8. Results for the pore-scale multispecies biofilm model in step 3.

4) We developed a multi-species biofilm model that considers direct electron transfer in the biofilm. Two common ways of electron transfer are inter-species electron transfer and direct electron transfer. The pore-scale multispecies biofilm model in task 3 considers inter-species electron transfer. In task 4, we developed a one-dimension multispecies biofilm model that considers direct electron transfer. Direct electron transfer occurs through nanowires in the biofilm. The model has four types of biomass, including syntrophs, DMRB, inert biomass, and extracellular polymeric substances (EPS), and six chemical species, including five dissolved species (propionate, H_2, acetate, U(VI), and ferrous ion (Fe^{2+})) and one solid species (goethite (FeOOH)).

Modeling Work: Hybrid multiscale methods that combine pore and continuum scales

We developed a hybrid model that combines the pore-scale multispecies biofilm model in step 3 to a continuous model. While pore-scale models represent high accuracy, they require detailed geometry input and are computationally expensive. Continuous models, on the contrary, do not require detailed geometry input and are computationally less demanding, but they generally have low accuracy for the types of problems considered here where resolution of sub-grid scale processes are important to compute overall reaction. Hybrid models combine the advantages from both sides. We divide the domain into two sub-domains: the continuous sub-domain and the pore-scale sub-domain. Figure 9 shows the problem setup. The electron donor is input in the top half of the domain through the left boundary, while the acceptor is input along the bottom half. Where these reactants mix, biofilm forms and clogs the pore space.
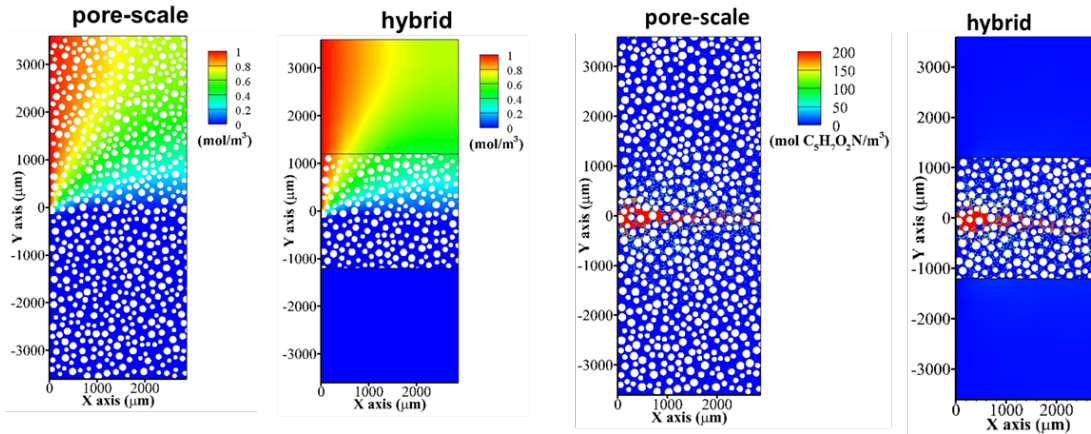

Figure 9. Comparison of the full pore-scale simulation with the hybrid continuum-pore method. The left shows the concentration of the electron donor after 27 days; the right shows the biofilm concentration.

The hybrid scheme ensures continuous concentration and flux at the boundaries that separate the continuous sub-domain from the pore-scale sub-domain. We have developed a hybrid model that considers diffusion and reaction. We used Mortars as the hybrid method. Figure 10 shows that the biomass accumulation is similar for the hybrid model and the pore-scale model. These findings are reported in Tang et al. (2015).
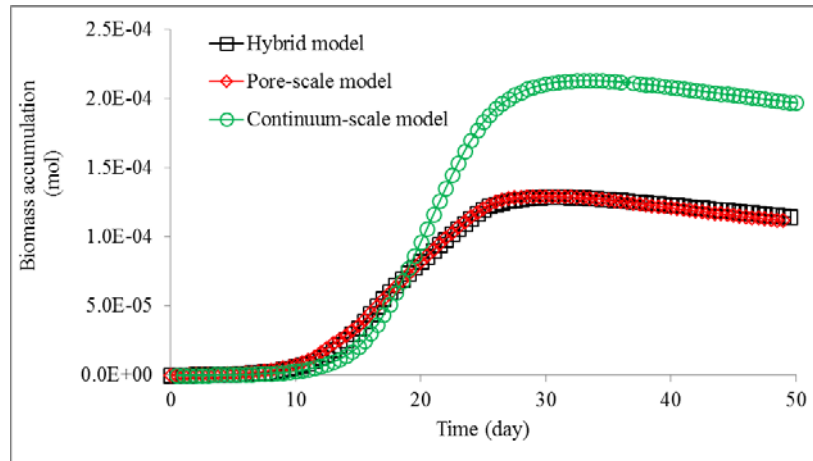

Figure 9. Simulated biomass accumulation in the flow domain.

Modeling work: A hybrid multi-time-step coupling of finite element and lattice Boltzmann methods with non-matching grids

Reactive flow and transport processes in porous media exhibit multiple time- and length-scales. Some of these processes (e.g., precipitation and dissolution) can even alter the pore structure. Continuum models may not be able to adequately capture the phenomena that occur at the pore-scale. This serves as a strong motivation for the development of hybrid multi-scale computational methods, which are aimed at providing an ideal setting to incorporate features and describe processes at different scales. However, capturing disparate temporal and spatial scales still remains an enduring challenge in computational mathematics. No single numerical method can efficiently bridge the gap between these disparate scales. Hence, designing numerical methodologies that employ different numerical methods in different regions has grown into a major topic of interest among researchers. Under this research program, a computational framework that couples the finite element method with the *entropic* lattice Boltzmann method for advection-diffusion equations has been developed. This framework allows non-matching grids, which facilitates to capture disparate spatial scales. Furthermore, under the proposed method, the finite element and lattice Boltzmann methods can be integrated using different times-steps. Furthermore, new methods for enforcing macroscopic (Dirichlet and Neumann) boundary conditions for the lattice Boltzmann method that satisfy monotonicity in production of entropy has been introduced. Several numerical examples have been generated to show the application of the proposed methodology to transport phenomena in heterogeneous porous media. This work will be reported in a future publication (Karimi and Nakshatrala, under preparation).

Modeling Work: A numerical framework for diffusion-controlled bimolecular-reactive systems to enforce maximum principles and the non-negative constraint

We developed a novel computational framework for diffusive-reactive systems that satisfies the non-negative constraint and maximum principles on general computational grids. The governing equations for the concentration of reactants and product are written in terms of tensorial diffusion-reaction equations. We restricted our studies to fast irreversible bimolecular reactions. If one assumes that the reaction is diffusion-limited and all chemical species have the same diffusion coefficient, one can employ a linear transformation to rewrite the governing equations in terms of *invariants*, which are unaffected by the reaction. This results in two uncoupled tensorial diffusion equations in terms of these invariants, which are solved using a novel non-negative solver for tensorial diffusion-type equations. The concentrations of the reactants and the product are then calculated from invariants using algebraic manipulations. The novel aspect of the proposed computational framework is that it will always produce physically meaningful non-negative values for the concentrations of all chemical species. Several representative numerical examples are presented to illustrate the robustness, convergence, and the numerical performance of the proposed computational framework. We also compared the proposed framework with other popular formulations. In particular, we have shown that the Galerkin formulation (which is the standard single-field formulation) does not produce reliable solutions, and the reason can be attributed to the fact that the single-field formulation does not guarantee non-negative solutions. We have shown that the clipping procedure (which produces non-negative solutions but is considered as a variational crime) does not give accurate results when compared with the proposed computational framework. This part of the research work has been published in Nakshatrala et al. (2013)

LIST OF PUBLICATIONS
Subsurface Biogeochemical Research Program
DE-SC0006771

Microbiological-enhanced mixing across scales during *in-situ* bioreduction of metals and radionuclides at Department of Energy Sites

A. J. Valocchi (PI), C.J. Werth *(now at Univ Texas, Austin)*, W-T. Liu, R. Sanford, *U.of Illinois Urbana-Champaign*, K. Nakshatrala*, U. of Houston*

2013

Tang, Y. and A.J. Valocchi. 2013. An improved cellular automaton method to model multispecies biofilms. *Water Research*. doi: 10.1016/j.watres.2013.06.055

Nakshatrala, K., M.K. Mudunuru, and A.J. Valocchi. 2013. A numerical framework for diffusion-controlled bimolecular-reactive systems to enforce maximum principles and the non-negative constraint. *Journal of Computational Physics*. **253**: 278-307. ISSN 0021-9991. http://dx.doi.org/10.1016/j.jcp.2013.07.010

Tang, Y., A.J. Valocchi, C.J. Werth, H. Liu. 2013. An improved pore-scale biofilm model and comparison with a microfluidic flow cell experiment. *Water Resources Research*. **49**:8370-8382; doi:10.1002/2013WR013843

Nakshatrala, K. B., and D.Z. Turner. 2013. A mixed formulation for a modification to Darcy equation based on Picard linearization and numerical solutions to large-scale realistic problems. *International Journal for Computational Methods in Engineering Science & Mechanics*, **14:** 524-541.

2014

Oostrom, M., Y. Mehmani, P. Romero-Gomez, Y. Tang, H. Liu, H. Yoon,Q. Kang, V. Joekar-Niasar, M.T. Balhoff, T. Dewers, E.A. Leist, N.J. Hess,W.A. Perkins, C.L. Rakowski, M.C. Richmond, J.A. Serkowski, C.J. Werth, A.J. Valocchi, T.W. Wietsma, and C. Zhang. 2014. Pore-scale and continuum simulation of solute transport micromodel benchmark experiments. *Computational Geosciences*. 10.1007/s10596-014-9424-0

Nobu, M.K., T. Narihiro, H. Tamaki, Y.-L. Qiu, Y. Sekiguchi, T. Woyke, et al. 2014. Draft genome sequence of *Syntrophorhabdus aromaticivorans* strain UI, a mesophilic aromatic compound degrading syntroph. *Genome Announc*. 2, no. 1 e01064-13

Nobu, M.K., T. Narihiro, C. Rinke, Y. Kamagata, S.G. Tringe, T. Woyke, and W-T Liu. 2014. Microbial dark matter ecogenomics reveals complex synergistic networks in a methanogenic bioreactor. *The ISME Journal*. doi: 10.1038/ismej.2014.256

Nobu, M.K., T. Narihiro, T. Hideyuki, Y.L. Qiu, Y. Sekiguchi, T. Woyke, et al. 2014. The genome of *Syntrophorhabdus aromaticivorans* strain UI provides new insights for syntrophic aromatic compound metabolism and electron flow. *Environ Microbiol*. doi: 10.1111/1462-2920.12444

2015

Tang, Y., A.J. Valocchi, and C.J. Werth. 2015a. A hybrid pore-scale and continuum-scale model for solute diffusion, reaction, and biofilm development in porous media. *Water Resources Research*. **51**; doi:10.1002/2014WR016322

Tang, Y., C.J. Werth, R.A. Sanford, R. Singh, K. Michelson, M. Nobu, W. Liu, and A.J. Valocchi. 2015b. Immobilization of selenite via two parallel pathways during in situ bioremediation. *Environ Sci Technol.* **49:**4543-4550; doi:10.1021/es506107r

Hirani, A. N., K. B. Nakshatrala, and J. H. Chaudhry. 2015. Numerical method for Darcy flow derived using Discrete Exterior Calculus. International Journal for Computational Methods in Engineering Science and Mechanics, **16:** 151-169.

Under review

Shabouei, M., and K. B. Nakshatrala. On mechanics-based *a posteriori* **criteria to assess accuracy of numerical solutions for Darcy and Darcy-Brinkman equations,** *under review*, 2015. *[An e-print available on arXiv.]*

Chang, J., S. Karra, and K. B. Nakshatrala. Large-scale optimization-based non-negative computational framework for diffusion equations: Parallel implementation and performance studies, *under review*, 2015. *[An e-print available on arXiv.]*

Under preparation
Karimi, S., and K. B. Nakshatrala. A hybrid multi-time-step coupling of finite element and lattice Boltzmann methods with non-matching grids, *under preparation*.